Preparation, Stability, and In Vitro Performance of Vesicles Made with Diblock Copolymers

James C-M. Lee,[1] Harry Bermudez,[1] Bohdana M. Discher,[1] Maureen A. Sheehan,[1] You-Yeon Won,[2] Frank S. Bates,[2] Dennis E. Discher[1]

[1]*School of Engineering and Applied Science, University of Pennsylvania, Philadelphia, PA 19104; telephone: 215-898-4809; fax: 215-573-6334; e-mail: discher@seas.upenn.edu*
[2]*Department of Chemical Engineering and Material Science, University of Minnesota, Minneapolis, MN 55455*

Abstract: Vesicles made completely from diblock copolymers—polymersomes—can be stably prepared by a wide range of techniques common to liposomes. Processes such as film rehydration, sonication, and extrusion can generate many-micron giants as well as monodisperse, ~100 nm vesicles of PEO-PEE (polyethyleneoxide-polyethylethylene) or PEO-PBD (polyethyleneoxide-polybutadiene). These thick-walled vesicles of polymer can encapsulate macromolecules just as liposomes can but, unlike many pure liposome systems, these polymersomes exhibit no in-surface thermal transitions and a subpopulation even survive autoclaving. Suspension in blood plasma has no immediate ill-effect on vesicle stability, and neither adhesion nor stimulation of phagocytes are apparent when giant polymersomes are held in direct, protracted contact. Proliferating cells, in addition, are unaffected when cultured for an extended time with an excess of polymersomes. The effects are consistent with the steric stabilization that PEG-lipid can impart to liposomes, but the present single-component polymersomes are far more stable mechanically and are not limited by PEG-driven micellization. The results potentiate a broad new class of technologically useful, polymer-based vesicles. © 2001 John Wiley & Sons, Inc. *Biotechnol Bioeng* **73**: 135–145, 2001.
Keywords: vesicle; liposome; polymer; diblock; membrane

INTRODUCTION

Lipids are nature's own vesicle-forming amphiphiles. Although they assemble into semipermeable vesicles in aqueous solutions, their overall stability is intrinsically limited, often kinetically trapped (Lasic and Papahadjopoulos, 1998). Lipid membranes cannot, for instance, be strained without rupture, osmotically or otherwise, by more than about 5% in surface area (reviewed in Lipowsky and Sackmann, 1995; Needham and Zhelev, 1996). Furthermore, lipid membranes are susceptible to thermal transitions from gel to liquid crystalline phases. Such in-surface thermodynamic instabilities are critical determinants of overall membrane properties, including permeability (Bloom et al., 1991). Although modulators of membrane stability, particularly cholesterol, are well known for their interfacial action, all natural membrane systems also have a hydrophobic core thickness that lies in a very narrow range of 3–4 nm (Fig. 1) (Lipowsky and Sackmann, 1995). This thickness may be very well-suited for the insertion of natural membrane proteins, but it may not be so robust as a thicker, and therefore more cohesive and stable, hydrophobic core, as will be shown.

Certain limitations on biomembranes, as outlined above, raise questions as to the fundamental and intrinsic bounds on lamellar formation and stability. Indeed, for encapsulation technologies ranging from oral drug delivery (Okada et al., 1995) to environmental toxin sequestration (Henselwood et al., 1998), any enhancement of membrane stability can be of considerable benefit. Extended efforts to develop polymerizable lipids (e.g., O'Brien et al., 1985) reflect such motivations. However, in contrast to the postassembly stabilization achieved in laterally polymerized lipid systems, vesicles can also be formed in aqueous solutions from organic "super"-amphiphiles such as block copolymers (Cornelissen et al., 1998; Discher et al., 1999). A PEO-PEE diblock (Fig. 1) introduced by Hillmeyer and Bates (1996), specifically EO_{40}-EE_{37} (designated OE7; see Table I), has been shown to self-assemble into membranes that are hyperthick compared to any natural lipid membrane and are also an order of magnitude or more tougher (Discher et al., 1999). A novel PEO-PBD diblock, EO_{26}-BD_{46} (designated OB2), is shown here also to be capable of making vesicles (Fig. 1). Importantly, both OE7 and OB2 have mean molecular weights in excess of several kilodalton—much

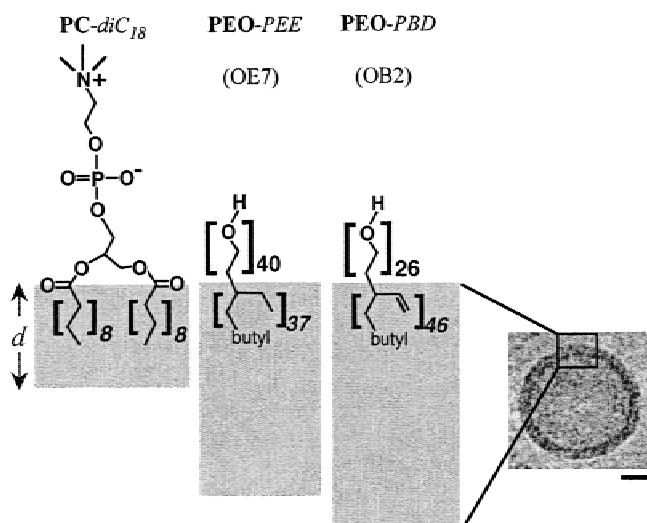**Figure 1.** Vesicle-forming amphiphiles. At far left is the structure of a typical diacyl chain lipid with a zwitterionic phosphatidylcholine (PC) head group. To the right are the structures of OE7 (PEO-PEE) and OB2 (PEO-PBD); see Table I for additional details. Hydrophobic fractions are indicated with italics. Membrane thickness, d, for each amphiphile is schematically illustrated with a gray bar. At far right is a cryo-TEM image of an OB2 vesicle; the scale bar is 20 nm.

larger than any natural membrane-forming amphiphile (Table I). Fuller characterizations of OE7 and OB2 vesicles, including some in vitro tests of compatibility, are our primary aim in this article.

As motivation, primary applications of liposomes are biomedical where their potential is rooted in the notion that natural lipids will be at least partially biocompatible (Lasic and Papahadjopoulos, 1998). However, it is also now well-appreciated that synthetic PEO and its structural equivalent PEG (polyethyleneglycol) generally enhance the compatibility of lipid membranes where these chains mimic the exofacial glycocalyx of cells. Indeed, so-called stealth liposomes are composed of phospholipids mixed with lipid-conjugated PEG in the molecular weight range of 1.5–5 kDa but at a mole fraction invariably much less than 25%. Although it is nebulous (Lasic and Papahadjopoulos, 1998) as to how PEG chains prolong circulation half-lives of liposomes from a few hours to tens of hours, the mechanism seems likely to involve minimizing cell adhesion to a foreign surface. More PEG-lipid would not necessarily provide further benefit, but it does appear clear that higher PEG densities are not easily achieved in lipid vesicles. This is

because PEG-lipids have a thermodynamic tendency to form micelles (Bedu-Addo et al., 1996), as readily understood from the disproportionately large hydrophilic (PEO) headgroup (Israelachvili, 1991). To counter this, the hydrophobic moment needs to be made much larger; synthetic copolymers make this possible.

Both the saturated PEO-PEE and the unsaturated PEO-PBD chains have average hydrophobic weight fractions (Table I) in the weight range typical of natural membrane-forming phospholipids, i.e., 60–80%. Whether the molecularly dense brush of PEO chains in the assembled polymersomes imparts a suitable level of biocompatibility is a central issue to be addressed. Efficiencies of molecular encapsulation during polymersome formation are also of importance for applications and are therefore elaborated, although without extensive optimization.

Prior efforts at making polymer vesicles include those assembled from large block copolymers having small (<20%) hydrophilic fractions and made in organic solvents by slowly adding water (Zhang and Eisenberg, 1995; Yu and Eisenberg, 1998). In contrast, vesicles that form in strictly aqueous conditions, as liposomes and the present diblocks do, have also been reported with at least two other wholly synthetic polymers. Cornelissen et al. (1998) used polystyrene (PS) as a hydrophobic fraction in their series of chiral block copolymers designated PS_{40}-(isocyano-L-alanine-L-alanine)$_x$. For $x = 10$, but not $x = 20$ or 30, small collapsed vesicles with diameters ranging from tens of nanometers to several hundred and a bilayer thickness of 16 nm were mentioned as existing under acidic conditions. However, bilayer filaments and superhelical rods also existed under the same solution conditions, making uncertain the stability of the collapsed vesicles. The relatively common pluronic (EO_5-PO_{68}-EO_5; 10% PEO by weight) is another copolymer that was found recently by cryo-TEM to yield small, ~5 nm thick vesicles (Schillen et al., 1999). However, these pluronic vesicles have a half-life of only 2–3 h, which is a finding that probably reflects a more hydrophilic character to the nominally hydrophobic propyleneoxide-midblock. Both PEE and PBD in the diblocks studied here, are, in contrast, more hydrophobic, resulting in much greater vesicle stability, as will be shown.
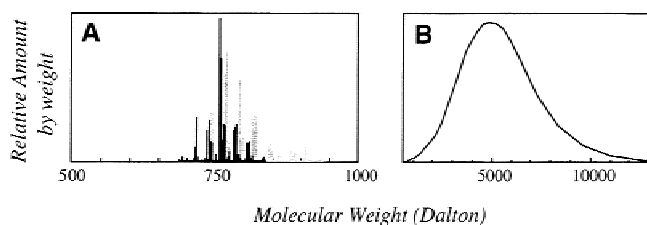
The results below are organized as follows. First, a diverse set of methods are demonstrated for making a broad range of polymer vesicle sizes. Then, making use of the largest, giant vesicles (diameters >1 μm), both unique and lipid-like membrane mechanical properties are measured and tabulated, showing little variation between methods as well as between the two copolymers. Polymersome stability is next elucidated in various media, including biological, and over a broad range of temperatures. Following these more physical tests, polymer vesicles are finally described as relatively inert in their in vitro interactions with living cells, both phagocytic and more quiescent cells. The results lead us to expect that many other polymers can and will be synthesized for the purposes of making unnaturally thick and robust biocompatible membranes.

Table I. Vesicle-forming polymers of PEO-PEE and PEO-PBD

Designation	Formula	Molecular weight[a]	f_{EO} (volume frcn.)	M_w/M_n[b]
OE7	EO_{40}-EE_{37}	3.9	0.39	1.10
OB2	EO_{26}-BD_{46}	3.6	0.28	1.07

[a]Number-average (M_n) in kilodaltons.
[b]Weight-average molecular weight: M_w.

MATERIALS AND METHODS

Polymers

EO$_{40}$-EE$_{37}$ (OE7) and EO$_{26}$-BD$_{46}$ (OB2) were synthesized according to Hillmyer and Bates (1996). The distribution of polymer molecular weights was determined by gel-permeation chromatography (GPC) in chloroform relative to polystyrene standards and is specified by the number average and weight-to-number average molecular weights of Table I. For completeness, the number average molecular weight for a discrete distribution of n different molecular weights is given by $M_n = \sum_{i=1}^{n} N_i M_i / \sum_{i=1}^{n} N_i$, where N_i is the number of molecules of mass M_i. Likewise, the weight average $M_W = \sum_{i=1}^{n} N_i M_i^2 / \sum_{i=1}^{n} N_i M_i$.

An important feature of the present synthetics—in comparison to natural lipids that make up biomembranes—is the width of their respective molecular weight distributions (Fig. 2). Figure 2A shows distributions, both measured and estimated, for some of the major phospholipids of the most commonly studied biomembrane, that of the red cell (Connor et al., 1997). Phosphocholines are the predominant phospholipids in this membrane at about 20% by total lipid weight, followed by sphingomyelin, phosphoethanolamine, and others. However, the two fatty acid chains in any given phospholipid can be very different and range from saturated 16-carbon chains to highly unsaturated 24-carbon chains. What results is a *finite* polydispersity in natural membranes which we calculate here for the measured phosphocholine together with phosphoethanolamine components to be $M_w/M_n \approx 1.001$. This is a lower bound which ignores not only the other uncharacterized phospholipids but also cholesterol (about 20% by weight of the membrane) and embedded integral membrane proteins, neither of which are membrane-forming amphiphiles in and of themselves. Nonetheless, a standard measure of width $w = (M_w/M_n - 1)^{1/2}$ indicates that the width of the OE7 distribution (Fig. 2B) normalized by its mean is about 10 times that of the illustrated natural phospholipid distributions. The robust tendency for OE7 to self-organize into vesicles despite the disparity in w is described below. Moreover, even more

polydisperse synthetic super-amphiphiles have been observed to form vesicles in water (Holder et al., 1998). The dispersion in these soft systems will be seen to self-average away. What results is not only reproducible collective behavior but also highly robust responses *not* dominated in any obvious ways by the extremes of the distribution.

Chemicals

Stock solutions of 1-stearoyl-2-oleoyl-glycero-3-phosphocholine (SOPC), 1,2-dimyristoyl-*sn*-glycero-3-phosphocholine (DMPC), both from Avanti Polar Lipid (Alabaster, AL), and 6-dodecanoyl-2-dimethylamino-naphthalene (LAURDAN) from Molecular Probes (Portland, OR) were made using chloroform. Phosphate-buffered saline (PBS) was prepared by dissolving PBS tablets from Sigma (St. Louis, MO) in deionized water. Sucrose in water (250–300 mOsm) was the typical media present during vesicle formation. Blood plasma was obtained from healthy donor blood centrifuged at 7,200g to sediment cells and then filtered through a 0.2 μm sterile syringe filter. Sodium citrate was used as an anticoagulant at the time of blood collection. Lyophilized horse heart myoglobin, lyophilized human hemoglobin, and bovine serum albumin (BSA) were from Sigma and used without further purification. Trypan blue (Sigma) was used in cell viability assays. All other chemicals were also purchased from Sigma.

Microscopy and Micromanipulation

Video microscopy was done with a Nikon TE-300 inverted microscope. A custom manometer with pressure transducers (Validyne, Northridge, CA) was used for controlling and monitoring the pressure applied to a micropipette. Imaging was generally done with either a 40×, 0.75 NA air objective lens under bright-field illumination or, for phase imaging, either a 10×, 0.3 NA or a 20×, 0.5 NA phase objective lens. Whereas bright-field microscopy enables visualization of the vesicle membrane (e.g., Fig. 3C), phase contrast is useful when a refractive difference is established between interior and exterior solutions (e.g., sucrose inside and PBS outside) which makes the vesicle appear phase dense (e.g., inset Fig. 4A). If a vesicle's membrane loses its integrity, the resulting exchange of solutes will moderate any phase contrast.

Preparation of Polymer Vesicles

Preparation of polymer vesicles was accomplished by either electroformation (Discher et al., 1999), film rehydration, or bulk rehydration. For film rehydration, 20 μL of 4.0 mg/ml of polymer in chloroform was uniformly coated on the inside wall of glass vial, followed by evaporation of the chloroform under vacuum for 3 h. Addition of sucrose solution (250–300 mOsm) led to spontaneous budding of vesicles off of the glass and into solution. For bulk rehydration, a few milligrams of solid polymer were placed in 1 ml of sucrose solution with overnight stirring.

Figure 2. Molecular weight distributions for natural and polymer membranes. **A**: The distribution of red cell phospholipids, phosphocholine, and phosphoethanolamine have been fully analyzed by Connor et al. (1997), leading to the mass distributions shown in black. Based on these data, probable distributions for sphingomyelin and phosphoserine species were estimated, as indicated in light gray. **B**: Measured distribution for the synthetic diblock copolymer OE7, for comparison.

Reduced vesicle sizes were obtained by sonication, freeze-thaw cycles, and/or extrusion. In sonication, a 4-ml vial coated with 1 mg of polymer and 1 ml of solution was submerged into the water bath of a sonicator (Fischer Scientific, Fair Lawn, NJ; Model FS20) for 15 min. Freeze-thaw was done by submerging a vial of suspended vesicles in liquid nitrogen. After spontaneous bubbling of liquid nitrogen subsided, the vial was transferred to a 50°C water bath. This was repeated three times. Extrusion was performed by introducing a vesicle suspension into a thermally controlled stainless steel cylinder connected to pressurized nitrogen gas. The vesicle solution was pushed through a 0.1 μm polycarbonate filter (Osmonics, Livermore, CA) supported by a circular steel sieve at the bottom of the cylinder, where the vesicle solution was collected after extrusion. This was typically repeated five times. The size distribution of vesicles was measured by dynamic light scattering (DLS) (DynaPro, Protein Solutions, Charlottesville, VA).

Thermal and Mechanical Measurements by Micropipette Methods

Mechanical properties such as the area elastic modulus and the critical areal strain of membrane rupture were measured by micropipette methods as reported previously (Discher et al., 1999). Briefly, mechanical measurements of vesicles were performed in an open-sided chamber formed with two coverslips and two spacers. A thermal chamber was custom-made for measurements of membrane thermal expansivity. The methods of analysis follow those outlined in Evans and Needham (1987). Properties of SOPC or DMPC vesicles reported here are in good agreement with those reported earlier.

Fluorescence Spectroscopy of LAURDAN in Membranes

A trace amount (0.001 mole%) of the polarity-sensitive probe, LAURDAN, was mixed with either polymer or lipid in chloroform followed by vesicle formation for spectroscopic study. The emission peak of LAURDAN in bilayer membranes is known to red-shift upon raising the temperature (Parasassi et al., 1991). A generalized polarization function (GP) of LAURDAN has been defined to capture this shift.

$$GP = \frac{I_B - I_R}{I_B + I_R}$$

where I_B and I_R are the emission intensities at λ_B and λ_R, and λ_B and λ_R are the emission peaks at 5°C and 60°C, respectively, when excitation is held fixed at 350 nm. For DMPC, λ_B and λ_R were found to be 442 nm and 485 nm, respectively. For OE7, λ_B was found to be 464 nm and λ_R was 475 nm. In this experiment, GPs of LAURDAN in OE7 and DMPC were obtained at different temperatures ranging from 5–60°C using an SLM2000 spectrofluorometer (Spectronic Instruments, Newark, DE).

Encapsulation of Proteins—Globins and BSA

Myoglobin was dissolved in 290 mOsm sucrose at 20 mg/ml for encapsulation during electroformation. Although proteins are generally more stable in buffered electrolytes, such solutions tend to inhibit electroformation of vesicles. Hemoglobin could not be encapsulated during electroformation; however, polymer vesicles could be formed during rehydration in a medium of 20 mg/ml hemoglobin in 140 mOsm sucrose solution plus 140 mOsm PBS. Similar procedures were also used for encapsulation of fluorescently labeled BSA into OE7 vesicle. The efficiencies of globin encapsulations were estimated by comparisons to bright-field images of red cells with adjustment for vesicle size. The encapsulation efficiency of fluorescein-BSA, as a percent of total mass added, was estimated by spectrofluorometry after extensive dialysis.

Biocompatibility of Polymersomes by Trypan Blue Assay

C_2C_{12} cells were obtained from American Type Culture Collection (ATCC, Manassas, VA) and cultured in DMEM (Life Technologies, Grand Island, NY) while incubated at 37°C, 10% CO_2. The percentage of cell survival, with or without added polymersomes, was estimated by Trypan blue exclusion (Wu et al., 1999).

RESULTS AND DISCUSSION

Preparation, Elasticity, and Rupture of Vesicles

Polymer vesicles were prepared and processed by a number of methods of varying prevalence in the field of liposomes. Figure 3A,B show giant vesicles of OE7 and OB2, respectively, spontaneously budding off of either rehydrated films or bulk copolymer. Similar images can be obtained during electroformation (Angelova et al., 1992) of OE7 in which thin films are formed on two parallel platinum wires by chloroform evaporation; an oscillating voltage of somewhat higher amplitude (10 V, 10 Hz) than that typically used for phospholipids such as SOPC (3 V, 1–10 Hz) is then applied to drive the budding process. The necessity of a higher driving voltage in electroformation likely reveals a higher lamellar viscosity. This is also manifested in relatively slowed dynamics of osmotically induced vesicle shape changes of the sort illustrated in Discher et al. (1999). Vesicle formation solutions, depending on the process used, can range from pure water to 250 mM sucrose or physiological PBS. Smooth, unfaceted contours throughout these processes and additional manipulations are consistent with a fluid phase membrane. Although unilamellar vesicles predominate in electroformed preparations, multilamellar vesicles that exhibit an enhanced edge contrast also have a tendency to form in the various methods.

A giant unilamellar vesicle of 5–50 μm in diameter, once formed and detached from the growth substrate, can be
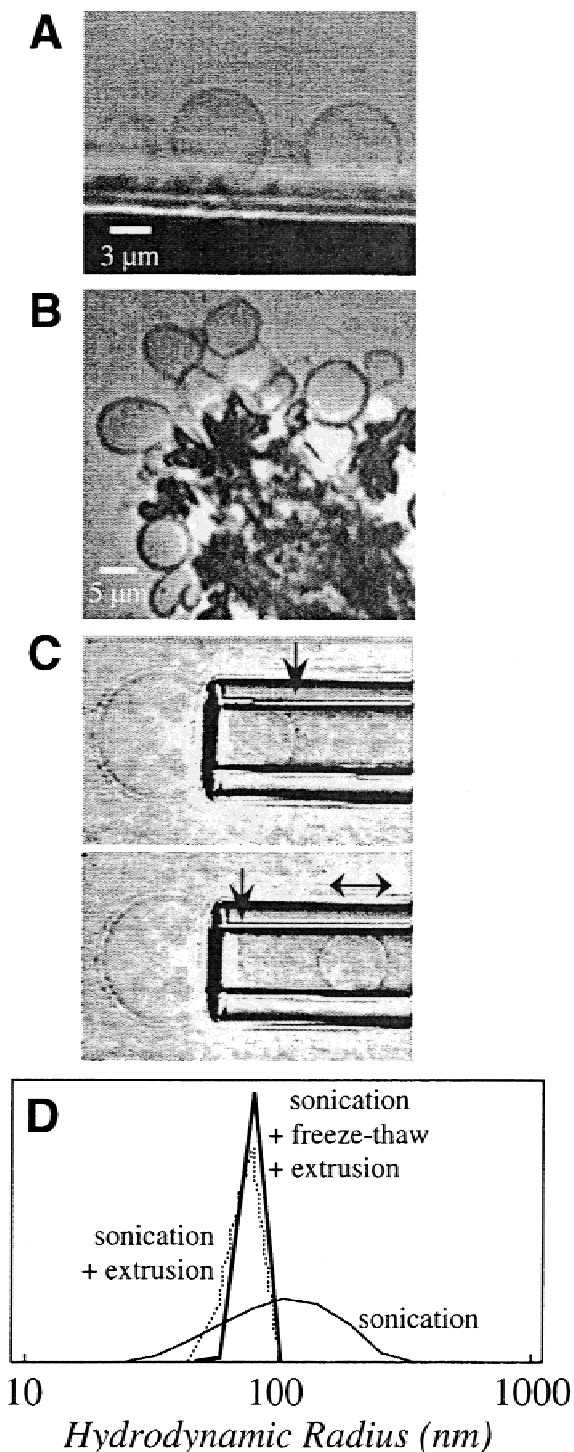
Figure 3. Polymersome preparation and fragmentation. **A**: Rehydration of a thin film of OE7 in 290 mOsm sucrose: polymersomes spontaneously form and bud off of the platinum surface. **B**: Rehydration of a micro-sliver of OB2 in 290 mOsm sucrose. **C**: Vesicle aspiration into a micropipette (6 μm bore), followed by fragmentation under a pressure transient. The vertical arrows point to the tip of the aspirated projections; the horizontal arrow matches the diameter of the vesicle fragment still connected to the vesicle body by a membrane tether. **D**: Polymersome (OE7) radii distributions after sonication (0.133 ± 0.065 μm), sonication plus extrusion (0.088 ± 0.013 μm), or sonication followed by freeze-thaw plus extrusion (0.093 ± 0.0086 μm), as assessed by DLS. Similar results were obtained for OB2.

made slightly flaccid by increasing the solution osmolarity, allowing the vesicle to be extended into a micropipette by aspiration (Fig. 3C, top). Like giant vesicles of lipid, these polymer vesicles can be fragmented as illustrated in Figure 3C by imposed pressure fluctuations. Under phase contrast rather than bright-field imaging, it is also clear that the vesicle's contents remain entrapped during vesiculation. Indeed, the passage of vesicles through a filter with pores of 0.1 μm diameter can be used, with or without sonication and freeze-thaw, to generate a very narrow distribution of vesicle sizes (Fig. 3D) with retained contents, as described further below.

The micropipette-aspirated length as a function of aspiration pressure reveals an essentially linear relation between the relative area expansion, α, and the imposed surface tension, τ, of these fluid phase vesicles (for calculations, see Discher et al., 1999). The slope of the fitted line corresponds to the area expansion modulus, $K_a = \tau / \alpha$, with units of interfacial tension. For lipid membranes this quantity has been reported to range from less than 100 mN/m to greater than 1,000 mN/m (reviewed in Needham and Zhelev, 1996). K_a is commonly viewed as related to the interfacial tension, γ, that is established on either side of the membrane and is in balance with molecular compression within the bilayer. A simple area elasticity calculation shows that $\gamma = 1/4 \, K_a$ (Israelachvili, 1991). Tabulation (Table II) of K_a for OE7 ($K_a \approx 120 \pm 20$ mN/m averaged over three formation processes) and OB2 ($K_a \approx 107 \pm 14$ mN/m) indicates not only that the unilamellar vesicles formed by the various processes tend to have a narrow range of reproducible K_a, but also that this basic interfacial elastic response is independent of the method used to form the vesicle.

The lack of any significant difference between the K_a's of OE7 and OB2 also suggests that the added double bonds of OB2 (Fig. 1) have little disordering effect. Lipids with multiply unsaturated acyl chains, in contrast, have been reported to give membranes with relatively lower K_a's (Needham and Zhelev, 1996). However, methyl groups protruding from the hydrocarbon chains of lipid (such as DPhPC: 1,2-diphytanoyl-*sn*-glycero-3-phosphocholine) are also well known to oppose close packing and thereby oppose gelation (e.g., Khan and Chong, 2000). The larger sidechains of OE7 and OB2 would likewise tend to dominate packing interactions and suppress freezing transitions; indeed, the glass transition temperature, T_g, is well below 0°C for bulk PEE as well as PBD. In a nanothin oriented film such as the membrane, polydispersity (Fig. 2B) also seems likely to add frustration to close-packing. The end result for these polymer membranes is an expectation that their hydrophobic cores are disordered fluids bounded by relatively diffuse, oil–water interfaces. The latter is concluded from the low values for γ of (≈ 30 for OE7 and ≈ 27 for OB2).

Given the large M_n of the present polymers compared to lipids, the elastic work to expand a membrane by a given increment certainly appears independent of M_n. This is, of course, consistent with the requisite work being interfacially localized at the hydrophobic–hydrophilic intersection, as

Table II. Formation methods and mechanical properties of vesicles.

Polymer or lipid	Method of formation	K_a (mN/m)[a]	$\alpha_c = (\Delta A/A_o)$[b]	d: thickness[c]
OE7	Electroformation	120 ± 20 [21 vesicles]	0.19 ± 0.02 [6 vesicles]	8 ± 1 nm
	Film Rehydration	115 ± 27 [20 vesicles]	0.20 ± 0.07 [5 vesicles]	
	Bulk Rehydration	123 ± 12 [4 vesicles]	0.27 ± 0.02 [3 vesicles]	
OB2	Bulk Rehydration	107 ± 14 [9 vesicles]	0.21 ± 0.02 [4 vesicles]	9 ± 1 nm
SOPC	Electroformation	171 ± 28 [3 vesicles]	0.05 [3 vesicles]	3–4 nm[d]

[a]K_a is the elastic modulus for area expansion.
[b]α_c is the critical area strain at which an initially unstressed membrane will rupture.
[c]Hydrophobic core thickness, d, is determined by cryo-TEM for the polymersomes.
[d]Typical range for all lipid membranes.

implied above. As an obvious corollary, the mean hydrophobic core thickness, d, would also appear to have little to no influence on surface elasticity. Indeed, despite a very narrow range of d for lipid membranes (Lipowsky and Sackmann, 1995), K_a has already been noted above to vary over an order of magnitude for lipid membranes. There are further implications in that there is a clear trend for lipid membrane permeability—which one generally desires to be low for drug delivery applications (Needham and Zhelev, 1996)—to increase in *inverse* proportion to K_a (Bloom et al., 1991); in other words, a lower γ means a more diffuse and permeated interface. In the case of the present polymersome membranes, however, the relatively low K_a is coupled with an enhanced thickness. This increased thickness disproportionately impedes transverse diffusion of water and directly translates into a considerably reduced hydraulic permeability compared to lipid membranes (Discher et al., 1999). Furthermore, the bending elastic constant, K_b, previously reported to be about 35 $k_B T$ (Discher et al., 1999) is extremely well-approximated by a model prediction of $\phi^{-1} K_a d^2$ with the coefficient $\phi = 48$ being derivable for a bilayer of two uncoupled monolayers (Bloom et al., 1991; Goetz et al., 1999). What thus seems most clear is that membrane thickness of these polymersomes allows for *differential* tuning of vesicle properties such as elasticity, permeability, and, as elucidated next, mechanical stability in ways not previously possible with lipid vesicles.

Indeed, despite lipid-like elasticities, the critical strain, α_c, of these polymer vesicles far exceeds the same metric of lipid membrane stability. Like bending and permeability this would also seem likely to have its origins in membrane thickness. Since K_a can be viewed as largely arising from γ of the hydrophobic-hydrophilic interface and should ordinarily be a critical determinant of cohesive strength or rupture, comparisons of α_c ought to be made with membranes having similar K_a. A 1:1 mixture of DAPC with cholesterol reportedly has a $K_a = 102$ mN/m (Needham and Nunn, 1990), and it has an $\alpha_c = 0.043$. If a critical yield stress (in mN/m^2) is postulated as common to both this lipid membrane and the tabulated polymersomes, then one might guess most simply that critical yield tensions as well as critical strains increase linearly with membrane thickness. Assuming that the ratio of hydrophobic thickness is the

determining factor, then the estimate for α_c appears low compared to the results listed in Table II; hydrophilic pores, wherein the polar (PEO) block rotates into the impending pore, would introduce an additional structural length scale. The PEO chain extends about 4 nm above (Won et al., 2000) each interface, whereas a lipid bilayer has a head-plus-tail thickness of 4–5 nm. With these $\alpha_c \sim 0.043$. (16/4) ~ 0.17, which is clearly much closer to the experimental values for polymersomes in Table II. A more systematic study of α_c's dependence on membrane thickness will appear elsewhere (Bermudez et al., in preparation).

Because of the evident similarity in mechanical properties between polymersomes prepared by various methods, no further process distinction is made in characterizations such as long-term stability (Fig. 4). In formal studies as well as more casual observation, it has been found that polymer vesicles in dilute suspension maintain their contents and a stable size distribution for a month or longer. In contrast, we find that giant SOPC vesicles suspended under the same conditions lose their phase contrast within a day: nominally, $\tau_{1/2} \sim 10$–20 h (Fig. 4B). Since the stability of a copolymer structure (Bates, 1991) such as the lamellar phase is well-appreciated as depending on the product of the Flory interaction energy, χ, and chain length, N, one would expect that the polymersomes are not only more stable mechanically but also that they have a much lower critical micellization concentration (CMC) than lipids, given the same χ. Importantly, since χ scales with γ (Helfand and Wasserman, 1982), comparisons such as this and others above between polymer and lipid membranes with similar K_a are generally valid.

Thermal Stability of Polymer Vesicles

The thermal response of lipid membranes, including gel-to-fluid surface transitions and microdomain formation, is extremely rich and can be both frustrating and useful to application. At boundaries between domains in a membrane, for instance, the permeability to solutes is invariably increased (Bloom et al., 1991). This can be used to enhance drug delivery in hyperthermic therapy (Needham et al., 2000), but leakiness can also make drug encapsulation inefficient if the surface transition is at or near the vesicle
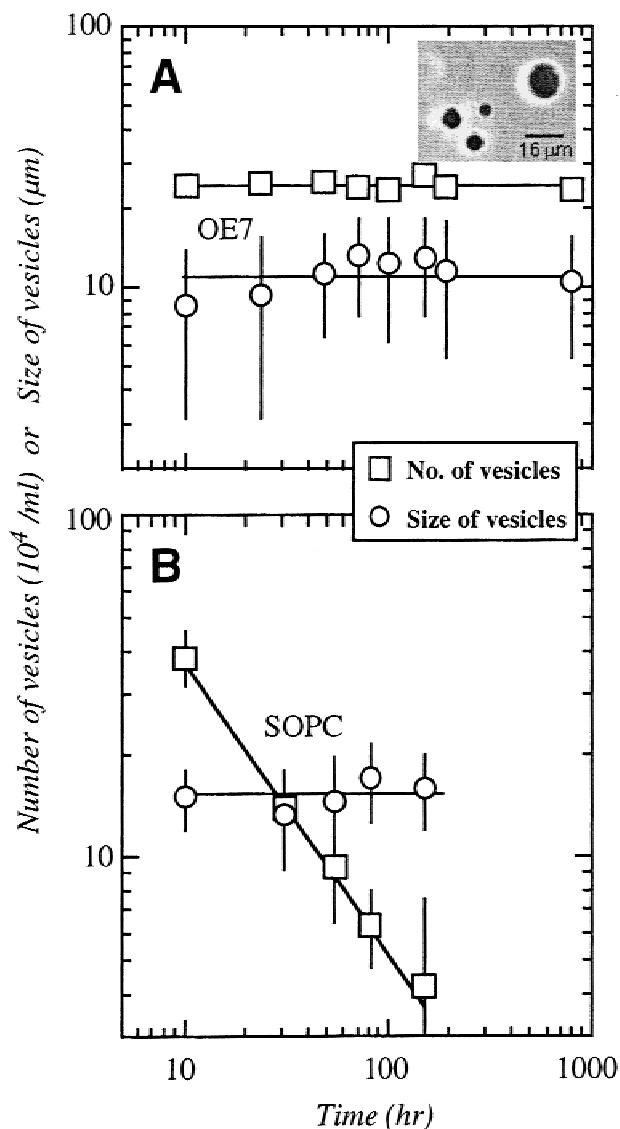
Figure 4. Stability of OE7 and SOPC vesicles in PBS. The vesicles contained 250 mOsm and therefore appear phase dense (inset), allowing those that retain their membrane integrity to be visually counted using a hemocytometer. **A**: With OE7 polymersomes, no significant changes in concentration or size distribution (20 random vesicles per point) were observed for at least a month. Similar stability has been noted for OB2 polymersomes. **B**: Phase contrast is lost from an increasing number of SOPC vesicles in an apparent power low decay process. The nominal half-life of the vesicles appears to be about 10–20 h, and the exponent for decay is fit with: number ~ time$^{\upsilon}$, with $\upsilon = 0.86$.

preparation or storage temperature. Since PEE is amorphous and predisposes a disordered melt for the core (Hillmyer and Bates, 1996), complex phase behavior is not to be anticipated through the typical freezing of the hydrophobic chains. Furthermore, although PEO has been reported to exist in semicrystalline states in pure diblocks having chain lengths similar to the ones analyzed here and at relatively moderate temperatures between 40°C and 70°C (Hillmyer and Bates, 1996), water is now known to swell the PEO chains even near the PEO–PEE/PBD interface (Won et al., 2000). This hydration and swelling would tend to amelio-

rate any PEO transition. In addition, the noted polydispersity of the diblocks making up the polymer membranes (Fig. 2B) would tend to blur and frustrate lateral ordering into any sort of nano-confined gel phase. With such factors in mind, both single vesicle and bulk techniques were employed in temperature scans of the polymersome membranes, particularly near the physiologically important range of 37°C.

First, by holding a single vesicle in a micropipette at a small but finite pressure and then increasing the ambient solution temperature, one generally observes a measurable expansion in the relative area of the vesicle membrane. For lipid membranes, far from a phase transition, the thermal expansion modulus, α_T, is generally in the range of 0.001–0.01/°C with a reference area conventionally taken near room temperature (Evans and Needham, 1987). Figure 5A,B compares the thermal area expansion of a polymersome membrane to that of a DMPC (lipid) membrane. Whereas a DMPC vesicle shows a dramatic change in area
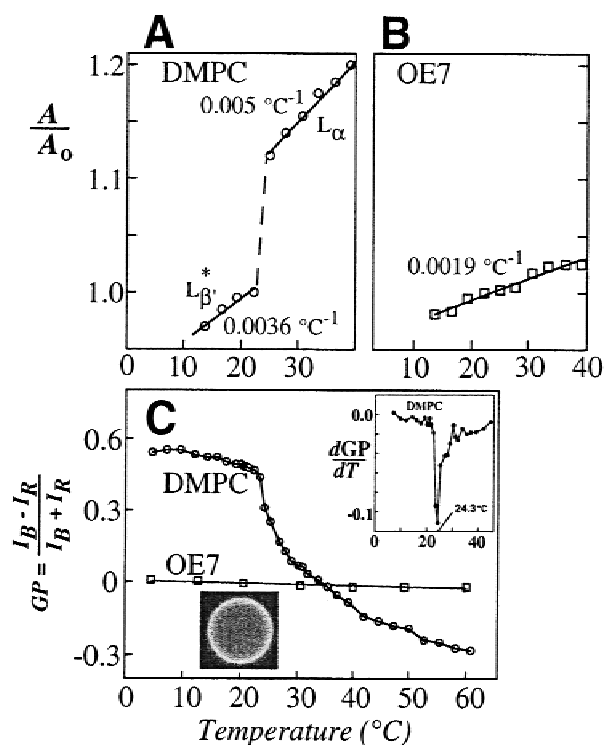
Figure 5. Thermally driven membrane area expansion and polarizability decrease. **A**: A single DMPC vesicle was held in a micropipette at a fixed tension of 2 mN/m, and the increase in its area was measured with increase in temperature. A large increase in membrane area is found near 24°C, consistent with previous reports for the main lamellar phase transition from L*$_{\beta'}$ to L$_{\alpha}$ (Evans and Needham, 1987). A more continuous thermal expansivity, α_T, is indicated both above and below this transition. **B**: Polymersomes of OE7 exhibit a smooth and gradual increase in membrane area with temperature, with no indication of a transition. A membrane tension of 4 mN/m was imposed. **C**: Spectrofluorometric probing of LAURDAN's generalized polarizability (GP) in bulk suspensions of DMPC or OE7 vesicles. LAURDAN was observed under the microscope to intercalate into both types of membranes (inset shows OE7 vesicle), but its spectral properties exhibit strong shifts with temperature only in DMPC vesicles near 24°C.

at a temperature between 23–25°C, as reported previously by Evans and Needham (1987), there is no similar gel-to-liquid discontinuity in the isobar for the polymersome membrane. This latter membrane simply expands with temperature at a rate of about 0.002/°C, which is comparable to longer chain lipid membranes like those composed of SOPC.

Results similar to those above were also arrived at in bulk suspension studies using the predominantly hydrophobic fluorophore LAURDAN. Fluorescence imaging of giant vesicles show that this probe is membrane localized (lower inset, Fig. 5C). With DMPC vesicles, a sharp drop in a suitable fluorescent blue-red intensity ratio, known as the generalized polarization or GP (see Methods), is seen once again at ~24°C, yielding a sharp peak in the slope $d(GP)/dT$ (upper inset, Fig. 5C). With polymersomes, there is only the smallest change in GP over a temperature range of 5–60°C. As will be elaborated elsewhere, the temperature-dependent change in wavelength shift can be used to explicitly calculate the local polarizability around the probe, and the change of this local polarizability with temperature, a thermal polarizability, correlates well with the thermal expansivity, α_T. Regardless, the spectroscopic results clearly indicate that the OE7 membranes possess no surface transitions, i.e., thermal instabilities, up to temperatures of at least 60°C.

At aqueous temperatures that approach boiling, certain lipid vesicle systems have previously been reported to exhibit surprising stability. These systems include archaelipids naturally designed for such purposes (Fan et al., 1995; Khan and Chong, 2000) as well as suspensions of small vesicles made with phosphocholines and containing minimal dissolved oxygen (Kikuchi et al., 1991; Zuidam et al., 1993). In the latter reference, autoclaving was explored as a means of sterilizing submicron vesicles that were too large for filtration through 0.22 μm filters. Vesicle diameter was found to be reduced and encapsulant leakage occurred, depending on the ionic nature of the lipid and encapsulant.

To press the thermal limits of polymersome stability, vesicles were autoclaved in dilute suspension for 15 min at a maximum cycle temperature of 121°C (2 atm). Under phase contrast, vesicles containing sucrose appear phase dense in PBS, allowing for visual determinations of number and size of intact giant vesicles. Table III shows that, after autoclaving, about 10% of the quasi-spherical vesicles have retained their contents and continue to appear phase dense.

However, the distribution of vesicle sizes shifts to a smaller and, perhaps surprisingly, tighter distribution. Clearly, thermal expansion would tend to generate excess membrane area which likely budded off, although without significant loss of encapsulated contents. Such fragmentation in the absence of frank lysis, as illustrated originally in Figure 3C, is readily understood, in principle, from a necking down and occlusion of the tether connecting to the small bud. Encapsulated solutes are neither lost nor gained to any significant extent in such a process. The clear implication is that there were many smaller budded but otherwise intact vesicles that could not be readily counted optically. Regardless of mechanism and considering only resolvable vesicles a few microns in diameter and larger, the decrease in average polymersome diameter corresponds to a retained volume of $\sim(50\%)^3 = 15\%$. Although seemingly inefficient, this unoptimized result may prove economical enough for sterilization, particularly if the freed encapsulant could be easily recycled.

Polymer Vesicles and Complex Solutions: Encapsulation Efficiency and Stability in Plasma

Complex solutions can modulate, in particular undermine, the stability of polymer vesicles through mechanisms such as alteration of γ. Indeed, difficulties in encapsulating globular proteins can arise with the surfactant-like character of denatured proteins, although the PEO brush of the present copolymers would tend to oppose interfacial access. Nonetheless, it is found that encapsulation within polymersomes can be as straightforward as adding solid pieces of bulk diblock to an aqueous solution of desired encapsulant and waiting 24 h. To develop a sense of encapsulation efficiency, three encapsulants were examined: myoglobin, hemoglobin, and albumin. All three could be entrapped during vesicle formation (Fig. 6), but with variable efficiency, as estimated by concentration or mass in Table IV. The efficiency of encapsulation, as well as its limitations, has as yet to be fully understood, but it is clear that encapsulation of macromolecules can be done with polymersomes.

More complex than a solution of a single protein, blood plasma has a number of surface-active agents, including
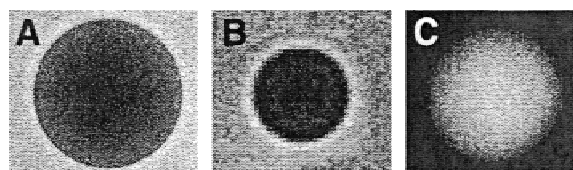
Figure 6. Encapsulation of proteins. **A**: A 15 μm diameter polymersome containing myoglobin. Encapsulation was accomplished during electroformation in 20 mg/mL myoglobin, 290 mOsm sucrose. **B**: A 5 μm polymersome containing hemoglobin. Encapsulaton was accomplished during film rehydration at 10°C in 20 mg/ml hemoglobin mixed into 140 mOsm PBS plus 140 mOsm sucrose solution. **C**: A 15 μm polymersome containing fluoresceinated-BSA, encapsulated as with hemoglobin, and observed by fluorescence microscopy.

Table III. Tabulation of phase dense vesicles after autoclaving (121°C, at 2 atm) for 15 min.

|	Before autoclave		After autoclave	
Trial #	No. of vesicles 10^4/ml	Size distribution (μm)	No. of vesicles 10^4/ml	Size distribution (μm)
1	82	7.3 ± 4.8	8	3.7 ± 0.4
2	94	6.0 ± 2.8	12	4.0 ± 0.6
3	121	8.2 ± 5.2	11	3.8 ± 0.5

Table IV. Encapsulation efficiency.

Encapsulant	Method	Bulk	Estimated encapsulated
Myoglobin	Electroformation	20 mg/ml	11 mg/ml
Hemoglobin	Film rehydration*	20 mg/ml	0.9 mg/ml
Fluor-albumin	Film rehydration	0.1 mg	0.005 mg (~5%)

*Shaking in 140 mOsm PBS, 140 mOsm sucrose at 10°C.

fatty acids and carrier proteins. In addition, such colloidal entities can generate osmotic depletion forces by becoming excluded from narrow gaps between juxtaposed membranes; surfactant bridging between adjacent vesicles can then act to more rigidly couple vesicles together. Stability in plasma thus has at least two aspects: membrane patency and colloidal stability. Figure 7A shows polymer vesicles to be
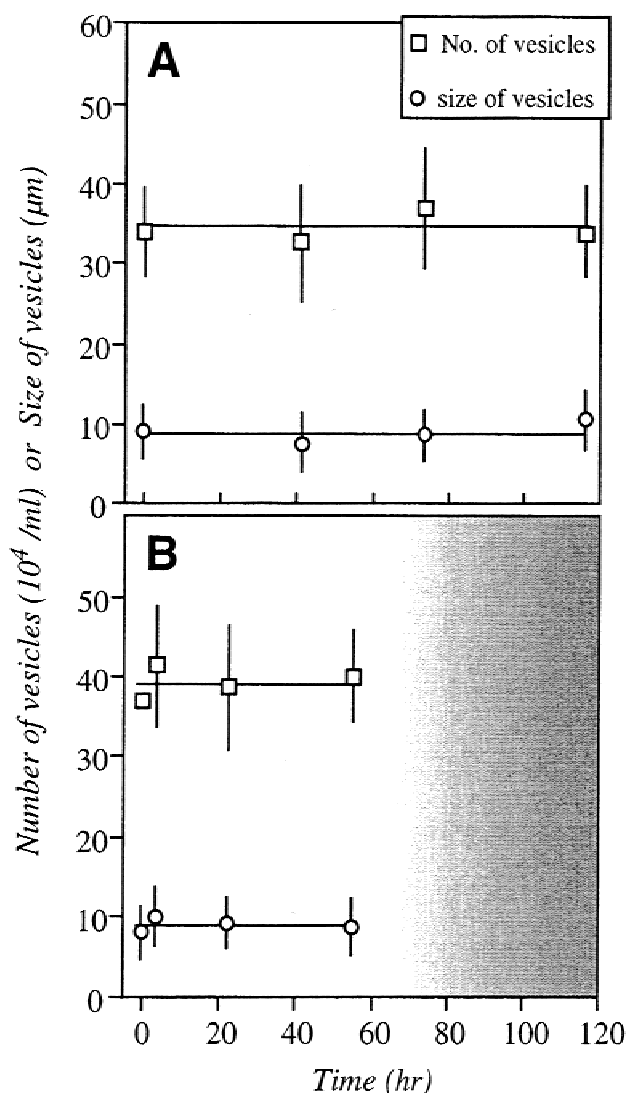
Figure 7. Polymersome stability in blood plasma. **A**: OE7 polymersomes suspended in PBS were added to an equal volume of fresh blood plasma and kept well-mixed with a tube rocker at room temperature. Vesicle number and size were stable for at least 5 days. **B**: In quiescent plasma, colloidal stability of polymersomes was observed out to 60 h. Aggregation of settled vesicles occurs after this.

stable for at least 5 days in plasma when suspended at room temperature and kept well-mixed in a quasi-physiological manner. Furthermore, Figure 7B demonstrates colloidal stability out to almost 60 h in quiescent plasma; frank aggregation of settled-out vesicles occurs at longer times. However, polymersomes in the formed aggregates do not appear to coarsen into either giant vesicles or bulk lamellar phases, despite the close proximity and elevated density in the aggregates. This indicates that polymer membrane fusion is not readily achieved—a finding most likely attributable to repulsion by the PEO brush. Nonetheless, the dense aggregates are not exceedingly fragile assemblies either, since they could not be sheared apart by rapid dragging through solution and generating surface shear stresses as high as ~1 dyne/cm^2. Regardless, the likelihood of forming such aggregates in vivo seems remote due to incessant fluid motion.
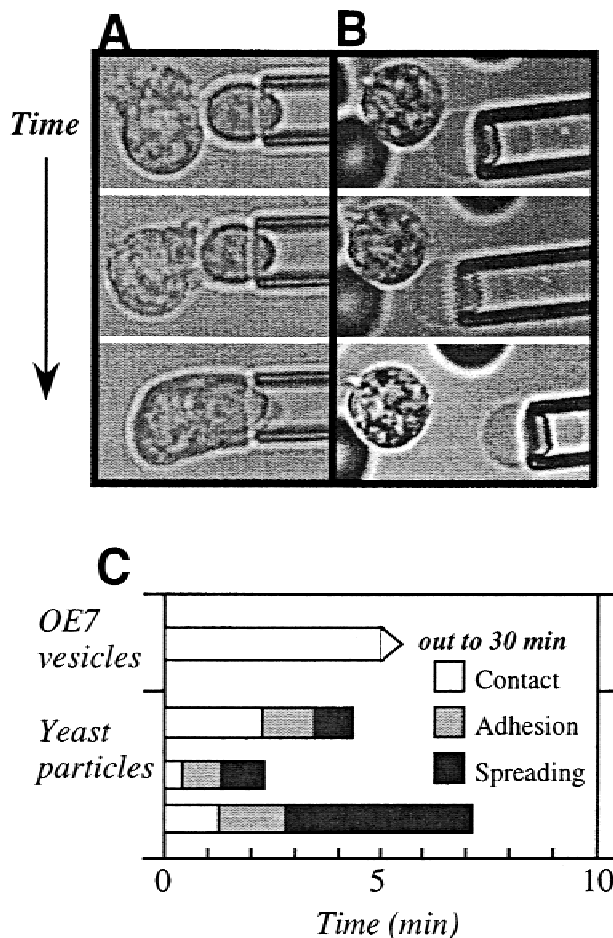
Phagocyte Challenge In Vitro

With polymersomes at least partially stable in blood plasma, a logical next step was to assess the interaction of a polymersome with the cellular components of blood, particularly granulocytes, which are the predominant circulating phagocytes. The basic in vitro experiment is illustrated in the video excerpts of Figure 8, which show either a yeast particle (Evans, 1989; Evans et al., 1993) or a polymersome being brought into contact with a blood cell. When in contact with red cells, neither polymersomes nor yeast particles exhibit any adhesion or other clear cellular response, despite the presence of 20% plasma. In comparison, within 1–2 min of a granulocyte contacting at least a yeast cell, a strong adhesive interaction invariably develops and the white cell soon begins to spread and actively engulf the yeast particle (Fig. 8A). This type of control experiment was generally complete within 3–4 min (n = 3 particles). In contrast, over the same length of time and much longer OE7 polymersomes appeared inert to the phagocytes (n = 5 vesicles) (Fig. 8B). Several such experiments are summarized in the timelines of Figure 8C. Results similar to those for OE7 were also found with OB2, at least out to 5–10 min, despite OB2's shorter PEO chain of only about 1 kDa.

The dense PEO brush of the polymersomes may be again acting like the glycocalyx on cellular exofaces, preventing the deposition of phagocytic ligands such as plasma C3b on the vesicle surface and/or repelling phagocyte adhesion. The in vitro protein-rejecting properties of PEO-coatings, including nanoparticles (Peracchia et al., 1999), are well appreciated (Lasic and Papahadjopoulos, 1998). Ultimately, the lack of polymersome recognition by phagocytes would seem important to prolonged circulation upon intravital injection.
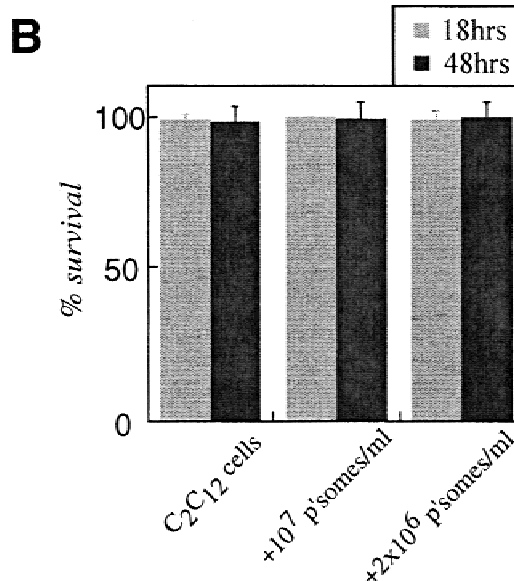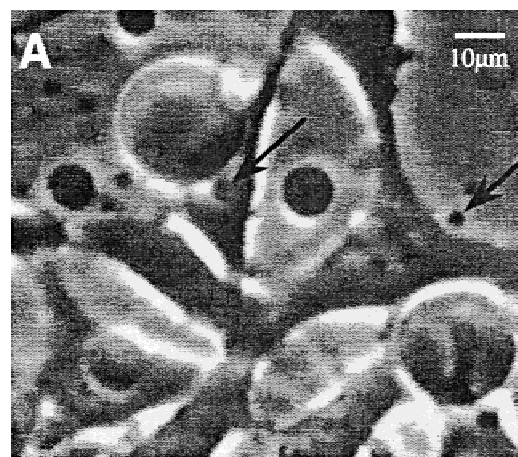
Biocompatibility in In Vitro Cell Culture

In a more prolonged model test of biocompatibility, non-differentiated C_2C_{12} cells were incubated with polymer-

Figure 8. Phagocyte challenge in vitro. Yeast particles (**A**) or OE7 polymersomes (**B**) were mixed in 20% citrated plasma and manipulated into contact with freshly washed granulocytic white blood cells and red blood cells. **C**: Within about 5 min white cells adhered to and engulfed the yeast particles, consistent with earlier studies (Evans, 1989). Polymersomes appeared inert in contact with a white cell for as long as 30 min. Interactions with red cells were nonexistent as well. The micropipette inner diameter is 5 μm. Experiments were done at room temperature and lasted 30–60 min.

Figure 9. Biocompatibility of polymersomes in vitro as assessed by cell viability. Before culturing, polymersomes were sterilized in 25% ethanol (v/v), exposed to UV light for 3 h, diluted with filtered PBS to an ethanol concentration of 6% v/v, and then added as half volume to culture dishes with subconfluent cells. Cells were preplated for 7 h to facilitate adhesion and spreading. **A**: Interactions between proliferating C_2C_{12} cells (at 18 h) and polymersomes, both small (arrows) and large, were clearly observable under phase contrast microscopy. By 48 h cultures were confluent. **B**: The percentage of surviving cells was assayed by Trypan blue exclusion and shows that polymersomes do not cause any ill-effect to living cells.

somes. The cells were first allowed to attach to culture dishes for several hours. Subsequently, a high concentration of small to giant sedimenting polymersomes were added to the cultures (Fig. 9A). In phase contrast, cells showed no signs of distress. In particular, they remained well spread with no evidence of membrane blebbing or cytotoxicity. There was also, however, no clear evidence of cellular import of polymer vesicles. After either 18 or 48 h, cell viability was assayed by Trypan blue exclusion. Despite the prolonged contact of the cells with the polymersomes under either subconfluent (18 h) or confluent conditions (48 h), there was no significant effect on cell survival (Fig. 9B). Results such as these with a myogenic cell line may prove directly relevant to nonviral gene therapy approaches to neuromuscular diseases. More generally, however, the results indicate no immediate toxic effect with intact PEO-PEE vesicles.

CONCLUSIONS

As preparation for more thorough in vivo evaluations of polymer vesicles, the present studies provide some indication of in vitro compatibility. Not only are proteins readily entrapped and plasma solutions withstood, but the polymersomes appear inert to white cells as well as adherent cultured cells. In addition, the polymer membranes appear thermally stable, with no transition-associated leaks to be anticipated. The results substantially reinforce the robust mechanical properties of variously prepared polymer vesicles compared to liposomes. Differences in physical

properties arise most logically with the increased membrane thickness and, perhaps, copolymer polydispersity since the hydrophobic-driving force for membrane assembly in water is generic to both super-amphiphilic diblocks and lipids. The new opportunities suggested for tailoring membrane properties such as stability might prove particularly crucial to success in particular applications where vesicles made with naturally occurring lipids prove far too unstable.

References

Angelova MI, Soléau S, Méléard Ph, Faucon JF, Bothorel P. 1992. Preparation of giant vesicles by external AC electric fields. Kinetics and applications. Progr Colloid Polym Sci 89:127–131.

Bates FS. 1991. Polymer-polymer phase-behavior. Science 251:898–905.

Bedu-Addo FK, Tang P, Xu Y, Huang L. 1996. Effects of polyethyleneglycol chain length and phospholipid acyl chain composition on the interaction of polyethyleneglycol phospholipid conjugates with phospholipid: implications in liposomal drug delivery. Pharm Res 13: 718–724.

Bloom M, Evans E, Mouritsen OG. 1991. Physical properties of the fluid lipid-bilayer component of cell membranes: a perspective. Q Rev Biopohys 24:293–397.

Connor WE, Lin, DS, Thomas G, Ey F, DeLoughery T, Zhu N. 1997. Abnormal phospholipid molecular species of erythrocytes in sickle cell anemia. J Lipid Res 38:2516–2528.

Cornelissen JJLM, Fischer M, Sommerdijk NAJM, Nolte RJM. 1998. Helical superstructures from charged poly(styrene)-poly(isocyanodipeptide) block copolymers. Science 280:1427–1430.

Discher BM, Won YY, Ege DS, Lee JC, Bates FS. Discher DE, Hammer DA. 1999. Polymersomes: tough vesicles made from diblock copolymers. Science 284:1143–1146.

Evans E. 1989. Kinetics of granulocyte phagocytosis: rate limited by cytoplasmic viscosity and constrained by cell size. Cell Motil Cytoskel 12:544–551.

Evans E, Needham D. 1987. Physical properties of surfactant bilayer membranes: thermal transitions, elasticity, rigidity, cohesion, and colloidal interactions. J Phys Chem 91:4219–4228.

Evans E, Leung A, Zhelev D. 1993. Synchrony of cell spreading and contraction force as phagocytes engulf large pathogens. J Cell Biol 122:1295–1300.

Fan Q, Relini A, Cassinadri D, Gambacorta A, Gliozzi A. 1995. Stability against temperature and external agents of vesicles composed of archael bolaform lipids and egg PC. Biochim Biophys Acta 1240:83–88.

Goetz R, Gompper G, Lipowsky R. 1999. Mobility and elasticity of self-assembled membranes. Phys Rev Lett 82:221–224.

Helfand E, Wasserman ZR. 1982. In: Developments in block copolymers-1 (Ch. 4) Goodman I, editor. New York: Applied Science Publishers.

Henselwood F, Wang GC, Liu GJ. 1998. Removal of perylene from water using block copolymer nanospheres or micelles. J Appl Polym Sci 70:397–408.

Hillmyer MA, Bates FS. 1996. Synthesis and characterization of model polyalkane-poly(ethylene oxide) block copolymers. Macromolecules 29:6994–7002.

Holder SJ, Hiorns RC, Sommerdijk NAJM, Williams SJ, Jones RG, Nolte RJM. 1998. The first example of a poly(ethylene oxide) poly(methyl-phenylsilane) amphiphilic block copolymer: vesicle formation in water. Chem Commun 14:1445–1446.

Israelachvili J. 1991. Intermolecular and surface forces, 2nd ed. New York: Academic Press.

Khan TK, Chong PL-G. 2000. Studies of archaebacxterial bipolar tetraether liposomes by perylene fluorescence. Biophys J 78:1390–1399.

Kikuchi H, Carlsson A, Yachi K, Hirota S. 1991. Possibility of heat sterilization of liposomes. Chem Pharm Bull 39:1018–1022.

Lasic DD, Papahadjopoulos D. 1998. Medical applications of liposomes. New York: Elsevier.

Lipowsky R, Sackmann E. 1995. Structure and dynamics of membranes — from cells to vesicles. Amsterdam: North-Holland.

Needham D, Nunn RS. 1990. Elastic-deformation and failure properties of lipid bilayer-membranes containing cholesterol. Biophys J 58: 997–1009

Needham D, Zhelev D. 1996. In: The mechanochemistry of lipid vesicles examined by micropipette manipulation techniques in vesicles (Ch. 9). Rosoff M, editor. New York: Marcel Dekker.

Needham D, Anyarambhatla G, Kong G, Dewhirst MW. 2000. A new temperature-sensitive liposome for use with mild hyperthermia: characterization and testing in a human tumor xenograft model. Cancer Res 60:1197–1201.

O'Brien DF, Klingbiel RT, Specht DP, Tyminski PN. 1985. Preparation and characterization of polymerized liposomes. Ann NY Acad Sci 446:282–295.

Okada J, Cohen S, Langer R. 1995. In vitro evaluation of polymerized liposomes as an oral drug delivery system. Pharm Res 12:576–582.

Parasassi T, Stasio G, Ravagnan G, Rusch RM, Gratton E. 1991. Quantitation of lipid phases in phospholipid vesicles by the generalized polarization of Laurdan fluorescence. Biophys J 60:179–189.

Peracchia MT, Harnisch S, Pinto-Alphandary H, Gulik A, Dedieu JC, Desmaele D, d'Angelo J, Muller RH, Couvreur, P. 1999. Visualization of in vito protein-rejecting properties of PEGylated stealth polycyanoacrylate nanoparticles. Biomaterials 20:1269–1275.

Schillen K, Bryskhe K, Mel'nikova YS. 1999. Vesicles formed from a poly-(ethylene oxide)-poly(propylene oxide)-poly(ethylene oxide) triblock copolymer in dilute aqueous solution. Macromolecules 32:6885–6888.

Won Y-Y, Davis HT, Bates FS, Agmalian M, Wignall GD. 2000. Segment distribution of the micellar brushes of poly(ethyleneoxide) via small-angle neutron scattering. J Phys Chem B 104:7134–7143.

Wu S, Li HY, Wong TM. 1999. Cardioprotection of precondition by metabolic inhibition in the rat ventricular myocyte: involvement of [kappa]-opioid receptor. Circ Res 84:1388–1395.

Yu K, Eisenberg A. 1998. Bilayer morphologies of self-assembled crew-cut aggregates of amphiphilic PS-b-PEO diblock copolymers in solution. Macromolecules 31:3509–3518.

Zhang LF, Eisenberg A. 1995. Multiple morphologies of crew-cut aggregates of polystyrene-b-poly(acrylic acid) block-copolymers. Science 268:1728–1731.

Zuidam NJ, Lee SSL, Crommelin DJA. 1993. Sterilization of liposomes by heat treatment. Pharm Res 10:1591–1596.